ACS OMEGA

Article

Cite This: ACS Omega 2019, 4, 8112−8121

http://pubs.acs.org/journal/acsodf

Exploring the Role of Consecutive Addition of Nitrogen Atoms on Stability and Reactivity of Hydrogen-Bonded Azine−Water Complexes

Neha Chopra,* Geetanjali Chopra, and Damanjit Kaur

Department of Chemistry, Guru Nanak Dev University, Amritsar 143005, India

Supporting Information

ABSTRACT: The second-order Møller−Plesset perturbation theory (MP2) and density functional theory with dispersion function calculations have been applied to investigate the hydrogen-bonding interaction between azines and water. The study suggests that the ability of nitrogen present in azine to act as a hydrogen-bond acceptor decreases in the order of pyridine (**PY**) > diazine (**DZ**) > triazine (**TZ**) > tetrazine (**TTZ**) > pentazine (**PZ**) > hexazine (**HZ**). Natural bond orbital (NBO) analysis, atoms in molecules, symmetry-adapted perturbation theory (SAPT), and molecular electrostatic potential studies reflect the factors important for hydrogen-bond strength as well as for the structural, electronic, and vibrational changes occurring during complexation. NBO analysis reflects that upon gradual addition of nitrogen atoms, hyperconjugation leads to an increase in the population of antibonding O−H bond, thus causing elongation and weakening of O−H bond in complexes incorporating N···H−O_W interaction, whereas rehybridization leads to an increase in the s character of the carbon hybrid orbital in C−H bond, thus causing contraction and shortening of C−H bond in complexes having C−H···O_W interactions. From the topological analysis, an excellent linear correlation is found to exist between stabilization energy (ΔE_{BSSE}), electron density (ρ_c), and its Laplacian ($\nabla^2\rho_c$) at the bond critical points.

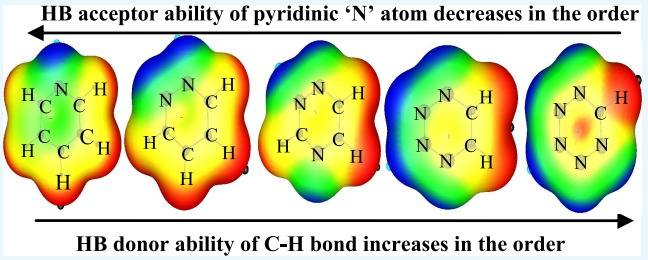

1. INTRODUCTION

Hydrogen-bonding interactions govern the pivotal role in monitoring the structural characteristics and function of biological molecules.[1,2] These hydrogen-bonding interactions are essential in protein folding, nucleobase stacking, DNA base-pairing, and enzyme catalysis.[3−7] Both conventional as well as unconventional hydrogen bonds (HBs) are important in determining the structure and reactivity of biological molecules. The conventional HB is defined as X−H···Y, where hydrogen atom lies between two electronegative elements, such as O, N, and F, whereas HBs are characterized as unconventional when C−H group is involved as an HB donor.[8] Strong conventional interaction of type N···H−O plays a significant role in controlling the conformation of small molecules, whereas unconventional C−H···O interactions play a dominant role in the stability of protein−protein interfaces, protein−ligand complexes, protein−nucleic acid interactions, and DNA−drug complexes.[9−14]

Among several biological active compounds, azines serve as a key building block for proteins, nucleotides, and polymers that play a pivotal role in biological and material science application. Hydrogen bonding involved in these species has reaped much more potential in medicinal chemistry,[15−22] and recently, several theoretical studies have been performed to analyze the effect of successive addition of nitrogen atoms in the biologically active heterocyclic aromatic moieties.[23−25] Azines are interesting model systems for investigating how successive replacement of C−H group with nitrogen atom affects the hydrogen-bonding ability of a 6-membered aromatic ring. Pyridine is found to have a large number of biological activities, including antiviral, anticancer, antimicrobial, antidiabetic, antitubercular, antidote, antileishmanial, antioxidant, antichagasic, antithrombin, anticoagulant, etc. along with most of the traditional biological activities.[26−29] Pyridazine (diazine 1,2) forms the skeleton of many drugs that are commercially available. Apresoline drug that contains pyridazine derivative treats hypertension in pregnant women. Azaphen is another pyridazine-based tricyclic antidepressant drug having sedative effects.[30−34] Pyrimidine (diazine 1,3) bases thymine, cytosine, and uracil subsume a pyrimidine pentagon ring fusion and are the most important building blocks of DNA and RNA.[35] Folic acid, thiamine, and riboflavin are some vitamins that contain the pyrimidine ring.[36−40] Triazine and tetrazine are highly electron-deficient aromatic systems due to abundance of electronegative nitrogen atoms. This property makes them sensitive toward various nucleophiles. The abundance of nitrogen atoms gives an advantage to use them in coordination chemistry. This property enables them to be used as templates for preparation of nanosize frameworks. Their derivatives are not only used for the treatment of a wide range of diseases but also for many more

Received: December 13, 2018
Accepted: April 9, 2019
Published: May 3, 2019

DOI: 10.1021/acsomega.8b03496
ACS Omega 2019, 4, 8112−8121

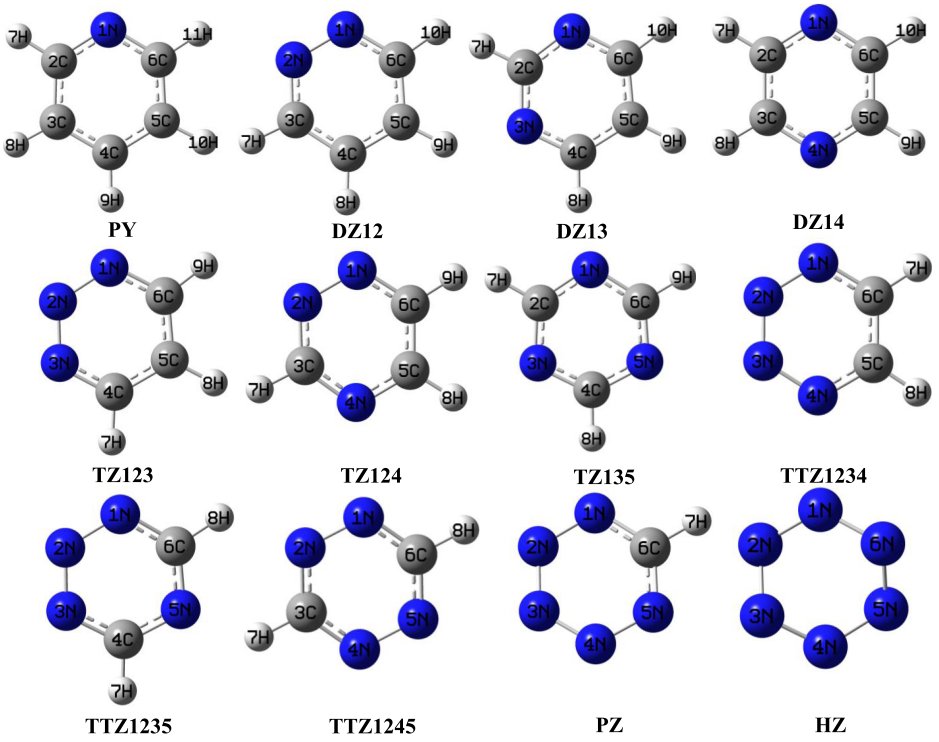

Figure 1. Optimized geometries of azines along with their isomeric forms at MP2/aug-cc-pVDZ level.

purposes, like in originating bactericides and fungicides, in oil fields as preservatives, disinfectants, industrial deodorants, etc.[41] Tetrazine-containing amino acids show tremendous stability in biological mediums and acidic solutions, which is one of the important criteria for cancer cell labeling and peptide modification.[42]

Hydrogen-bonding interactions involving hydrogen atoms positioned on azine ring are of particular interest because of the electron-withdrawing properties of azine. The hydrogens closely attached with aromatic azine rings are generally more electropositive than those attached with aliphatic azines, which leads to the formation of stronger H bonds. It is believed that aromatic units offer exclusive characteristics, which makes them differ from aliphatic interactions and thus can lead to specificity of structure and function.

A unified picture of azines interacting with water is presented in this manuscript. When azines interact with the hydrogen of water through nitrogen (N···H−O), a strong HB is formed, whereas C−H of azine donating HB to the oxygen of water (C−H···O) is considered to be a very weak interaction. The main purpose of conducting these studies is to gain insight into the strengths of these HBs as they relate to biologically relevant structures, especially protein−ligand complexes. The energetic, topological, electronic, and structural factors affecting the stability of hydrogen-bonded complexes of azine with water have been systematically analyzed.

2. RESULTS AND DISCUSSION

2.1. Stability and Structural Parameters. Pyridine (**PY**), diazine (**DZ**), triazine (**TZ**), tetrazine (**TTZ**), pentazine (**PZ**), and hexazine (**HZ**) have been optimized at wB97XD/aug-cc-pVDZ (L1) and MP2/aug-cc-pVDZ (L2) theoretical levels. As can be seen from Figure 1, **DZ12**, **DZ13**, and **DZ14** are isomeric forms of **DZ** with 1,2; 1,3; and 1,4 positioning of two N atoms, respectively. Similarly **TZ123**, **TZ124**, and **TZ135** are isomeric forms of **TZ** and **TTZ1234**, **TTZ1245**, and **TTZ1235** are isomeric forms of **TTZ**. The relative energy order of isomeric forms of **DZ**, **TZ**, and **TTZ** is as follows: **DZ12** < **DZ14** < **DZ13**, **TZ123** < **TZ124** < **TZ135**, and **TTZ1234** < **TTZ1245** < **TTZ1235**. It is observed that **DZ12**, **TZ123**, and **TTZ1234** are the least stable among their isomeric forms and have nitrogens adjacent to each other, which is in accordance with the anticipation. The hydrogen bonding of a single water molecule with these azines in the isolated state leads to stabilization energies that fall in the range −1.80 to −6.86 kcal/mol at L2 theoretical level whereas the range at L1 level falls from −1.24 to −6.62 kcal/mol. The optimized geometrical parameters for the complexes using L1 and L2 theoretical levels are summarized in Tables S5−S19. These hydrogen-bonded systems have been categorized on the basis of HB donor and acceptor groups in the complex form.

In type **WI** complexes (shown in Figure 2), the pyridinic nitrogen atom of azine is situated with its lone pair facing directly toward the hydrogen atom of water. These complexes involve single HB formation with N···H−O_W interaction. The order of stabilization energies in these complexes is as follows: **PY** > **TZ123** > **TTZ1234** ∼ **TTZ1235** > **PZ** > **HZ**, which shows that the tendency of pyridinic nitrogen atom of azine to act as a HB acceptor decreases with increase in the aza substitution. As displayed by structural parameters, the strength of N···H−O_W HB reduces with increase in the number of nitrogen atoms in the ring. The N···H−O_W HB angles in these complexes span the range 170−178°, which suggests the directionality of HB that provides a major contribution to the stability of complexes.

In type **WII** complexes (shown in Figure 2), water acts as a HB acceptor toward C−H of heterocyclic ring and HB donor toward N of the ring, resulting in a pseudo 5-membered ring. In these complexes, N···H−O_W has the major contributing interaction in ΔE_{BSSE} in comparison with C−H···O_W, as proposed by geometrical parameters. The stabilization energies

DOI: 10.1021/acsomega.8b03496
ACS Omega 2019, 4, 8112−8121

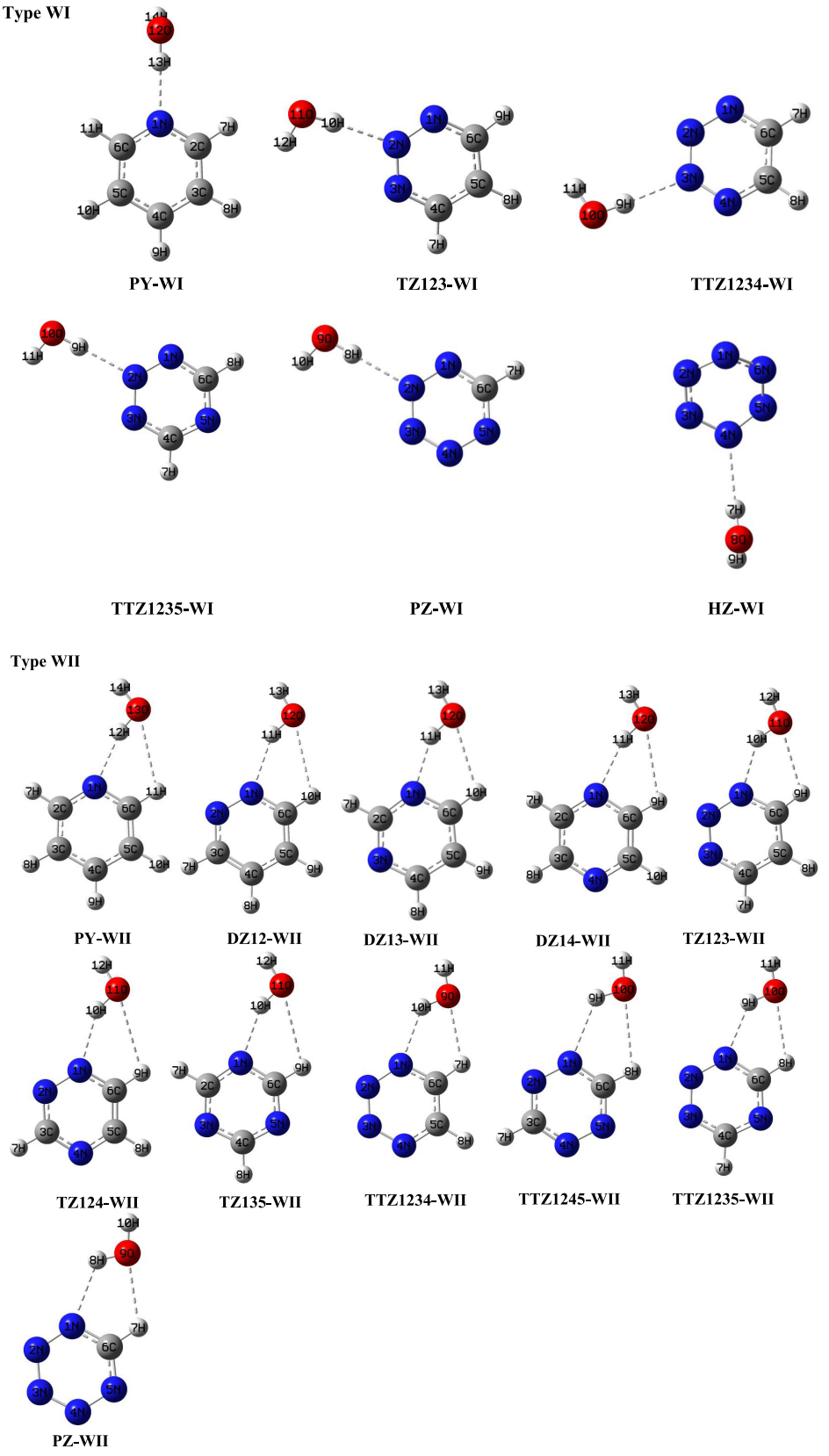

Figure 2. Optimized geometries of 1:1 hydrogen-bonded complexes of azines with water at MP2/aug-cc-pVDZ level (type **WI** and **WII**).

in these complexes authenticate the fact that the HB acceptor ability of the ring N atom decreases as the aza substitution increases. Complexes in which the basic center is directly bonded to the nitrogen atom, such as **DZ12-WII**, **TZ123-WII**, and **TTZ1234-WII**, have high stabilization energies in comparison with complexes in which the basic center is not directly bonded to the nitrogen atom, such as **DZ13-WII**, **DZ14-WII**, and **TZ135-WII**. The N···H−O_W HB angle in **WII**

DOI: 10.1021/acsomega.8b03496
ACS Omega 2019, 4, 8112−8121

Table 1. Hydrogen-Bond (HB) Distances r (in Å), Angles θ (in deg); Change in Bond Length Δd (in Å) and Shifts of Stretching Frequencies $\Delta\nu$ (in cm^{-1}) for the HB Donor Group (D−H) of Complexes of Azines with Water upon Complexation at MP2/aug-cc-pVDZ (L2) Level and BSSE-Corrected Stabilization Energies (ΔE_{BSSE} in kcal/mol) of Complexes at wB97XD/aug-cc-pVDZ (L1) and MP2/aug-cc-pVDZ (L2) Levels

types	complexes	HB distances	r (Å)	HB angles	θ (deg)	$\Delta\nu$	Δd	ΔE_{BSSE} (−ve) L1	ΔE_{BSSE} (−ve) L2
type **WI** (N···H−O_W)	**PY-WI**	H13···N1	1.9	O12−H13···N1	176	−262.37	0.019	6.27	6.34
	TZ123-WI	H10···N2	2.0	O11−H10···N2	176	−139.15	0.013	4.75	5.14
	TTZ1234-WI	H9···N3	2.1	O10−H9···N3	178	−92.10	0.011	3.90	4.18
	TTZ1235-WI	H9···N2	2.1	O10−H9···N4	178	−114.12	0.007	3.67	4.16
	PZ-WI	H8···N2	2.1	O10−H9···N4	171	−67.24	0.009	2.75	3.22
	HZ-WI	H7···N4	2.1	O8−H7···N4	170	−13.17	0.005	1.57	1.98
type **WII** (N···H−O_W and C−H···O_W)[a]	**PY-WII**	H12···N1	1.9	O13−H12···N1	156	−234.27	0.017	6.62	6.86
		O13···H11	2.7	C6−H11···O13	108	3.09	0.000		
	DZ12-WII	H11···N1	2.0	O12−H11···N1	150	−211.68	0.016	6.41	6.73
		O12···H10	2.6	C6−H10···O12	109	2.44	0.000		
	DZ13-WII	H11···N1	2.0	O12−H11···N1	150	−179.22	0.014	5.68	5.86
		O12···H10	2.6	C6−H10···O12	110	3.65	0.000		
	DZ14-WII	H11···N1	2.0	O12−H11···N1	152	−180.54	0.015	5.47	5.70
		O12···H9	2.7	C6−H9···O12	109	5.48	0.000		
	TZ123-WII	H10···N1	2.0	O11−H10···N1	142	−152.10	0.013	5.49	6.15
		H9···O11	2.5	C6−H9···O11	112	6.52	0.000		
	TZ124-WII	H10···N1	2.0	O11−H10···N1	146	−118.04	0.012	5.15	5.57
		H9···O11	2.6	C6−H9···O11	110	6.22	0.000		
	TZ135-WII	H10···N1	2.0	O11−H10···N1	146	−124.10	0.012	4.39	4.87
		H9···O11	2.6	C6−H9···O11	110	6.37	0.000		
	TTZ1234-WII	H10···N1	2.1	O10−H9···N1	132	−90.67	0.011	4.89	5.71
		H7···O9	2.4	C6−H8···O10	115	2.12	0.000		
	TTZ1245-WII	H9···N1	2.1	O10−H9···N1	136	−90.34	0.011	4.96	4.38
		H8···O10	2.5	C6−H8···O10	113	4.10	0.000		
	TTZ1235-WII	H9···N1	2.1	O10−H9···N1	136	−90.21	0.011	4.49	5.18
		H8···O10	2.5	C6−H8···O10	113	6.18	0.000		
	PZ-WII	H8···N1	2.2	O9−H8···N1	124	−44.38	0.008	4.77	4.95
		H7···O9	2.4	C6−H7···O9	116	9.48	0.000		
type **WIII** (two C−H···O_W)[a]	**PY-WIII**	H9···O12	2.6	C4−H9···O12	122	9.75	−0.001	1.24	2.10
		H10···O12	2.6	C5−H10···O12	121	9.75	−0.001		
	DZ12-WIII	H8···O11	2.6	C4−H8···O11	119	11.46	−0.001	1.98	2.84
		H9···O11	2.6	C5−H9···O11	120	11.46	−0.001		
	DZ13-WIII	H9···O11	2.5	C5−H9···O11	118	17.28	−0.001	3.47	2.61
		H10···O11	2.6	C6−H10···O11	119	20.07	−0.001		
	DZ14-WIII	H7···O11	2.6	C2−H7···O11	121	18.20	−0.002	1.58	2.15
		H8···O11	2.6	C3−H8···O11	121	18.20	−0.002		
	TZ123-WIII	H7···O10	2.6	C4−H7···O10	115	14.39	−0.001	3.16	3.50
		H8···O10	2.5	C5−H8···O10	122	14.39	−0.001		
	TZ124-WIII	H8···O10	2.6	C5−H8···O10	119	20.16	−0.002	2.36	3.26
		H9···O10	2.6	C6−H9···O10	119	20.16	−0.002		
	TTZ1234-WIII	H7···O9	2.5	C6−H7···O9	117	18.73	−0.002	3.31	4.20
		H8···O9	2.5	C5−H8···O9	117	18.73	−0.002		
type **WIV** (single C−H···O_W)	**PY-WIV**	H9···O12	2.3	C4−H9···O12	179	63.87	−0.007	1.62	1.80
	DZ12−WIV	H9···O11	2.2	C4−H9···O12	179	38.23	−0.007	2.28	2.76
	DZ13-WIV	H9···O11	2.2	C5−H9···O11	180	24.68	−0.006	2.14	2.50
	DZ14-WIV	H9···O11	2.2	C5−H9···O11	178	32.37	−0.007	1.81	1.86
	TZ123-WIV	H8···O10	2.2	C5−H8···O10	179	12.67	−0.006	3.35	3.48
	TZ124-WIV	H8···O10	2.2	C5−H8···O10	180	19.01	−0.005	2.80	2.98

[a]In type **WII** complexes, both $_W$O−H···N and C−H···O_W HBs and in type **WIII**, two C−H···O_W HBs contribute to ΔE_{BSSE} value of the complexes.

complexes is found to lie in the range of 124−156°. The deviation from 180° suggests the role of secondary C−H···O_W interaction present in the complexes.[43] The HB angles are quite linear in type **WI** complexes that are stabilized by a single HB, whereas the existence of a second HB in type **WII** complexes leads to formation of a pseudo 5-membered ring structure along with a heterocyclic ring, forcing the HB angle to be deviated from linearity. The type **WII** complexes are found to be 0.52−1.73 kcal/mol more stabilized in relation to their respective type **WI** complexes.

In type **WIII** complexes (shown in Figure S1), both lone pairs present in the oxygen of water act as a HB acceptor toward two

DOI: 10.1021/acsomega.8b03496
ACS Omega 2019, 4, 8112−8121

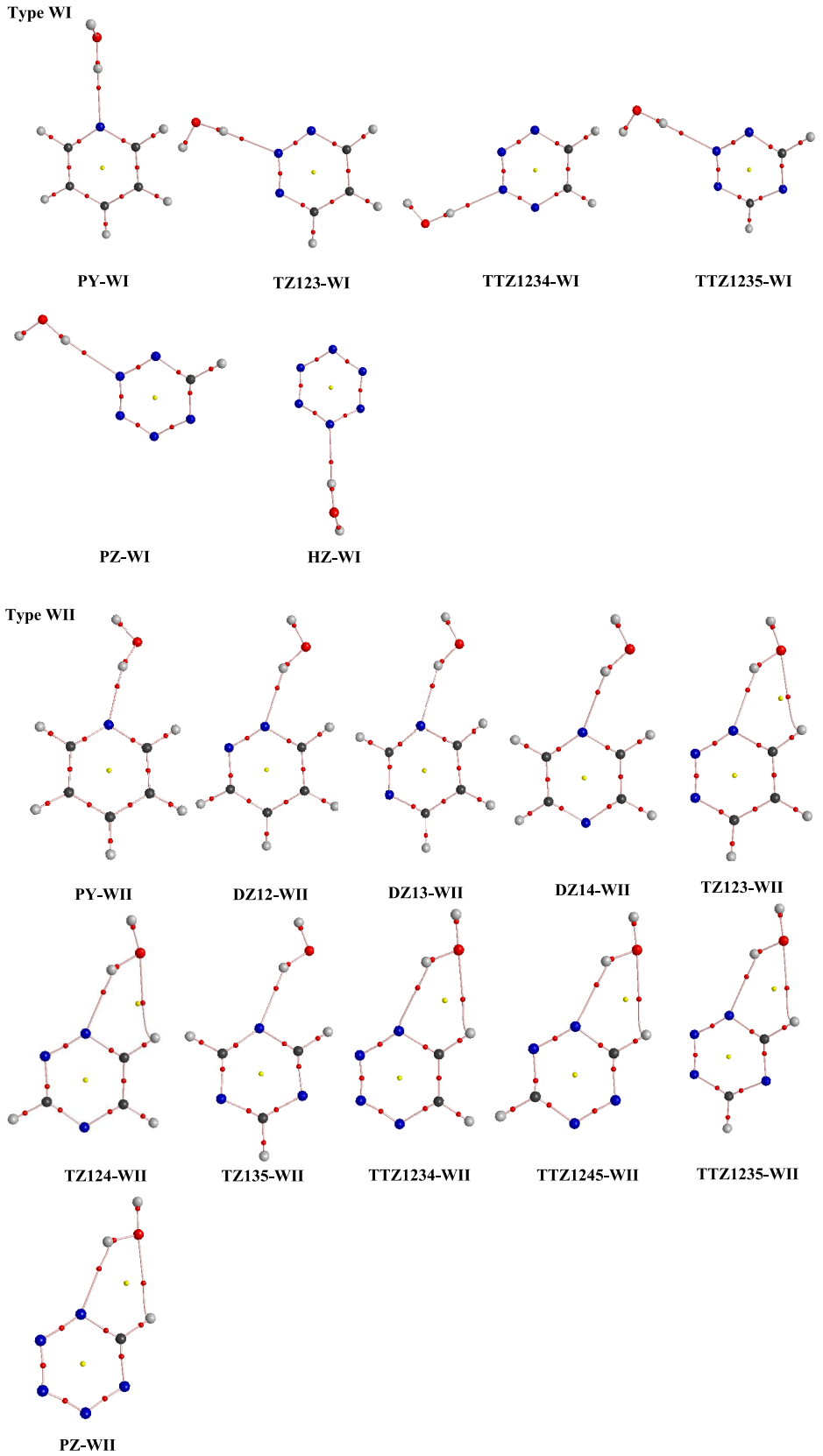

Figure 3. AIM molecular graphs of complexes of azines with water at MP2/aug-cc-pVDZ level (type **WI** and **WII**). Small red balls indicate bond critical points, and small yellow balls indicate ring critical points.

C−H bonds of azines. These complexes involve the formation of a bifurcated structure with water bonding to two C−H hydrogens. The order of stabilization energy in these complexes is as follows: **TTZ1234** > **TZ123** > **TZ124** > **DZ12** > **DZ13** > **DZ14** > **PY**, which indicates the fact that C−H HB donor ability decreases as the aza substitution decreases. The values of C−

DOI: 10.1021/acsomega.8b03496
ACS Omega 2019, 4, 8112−8121

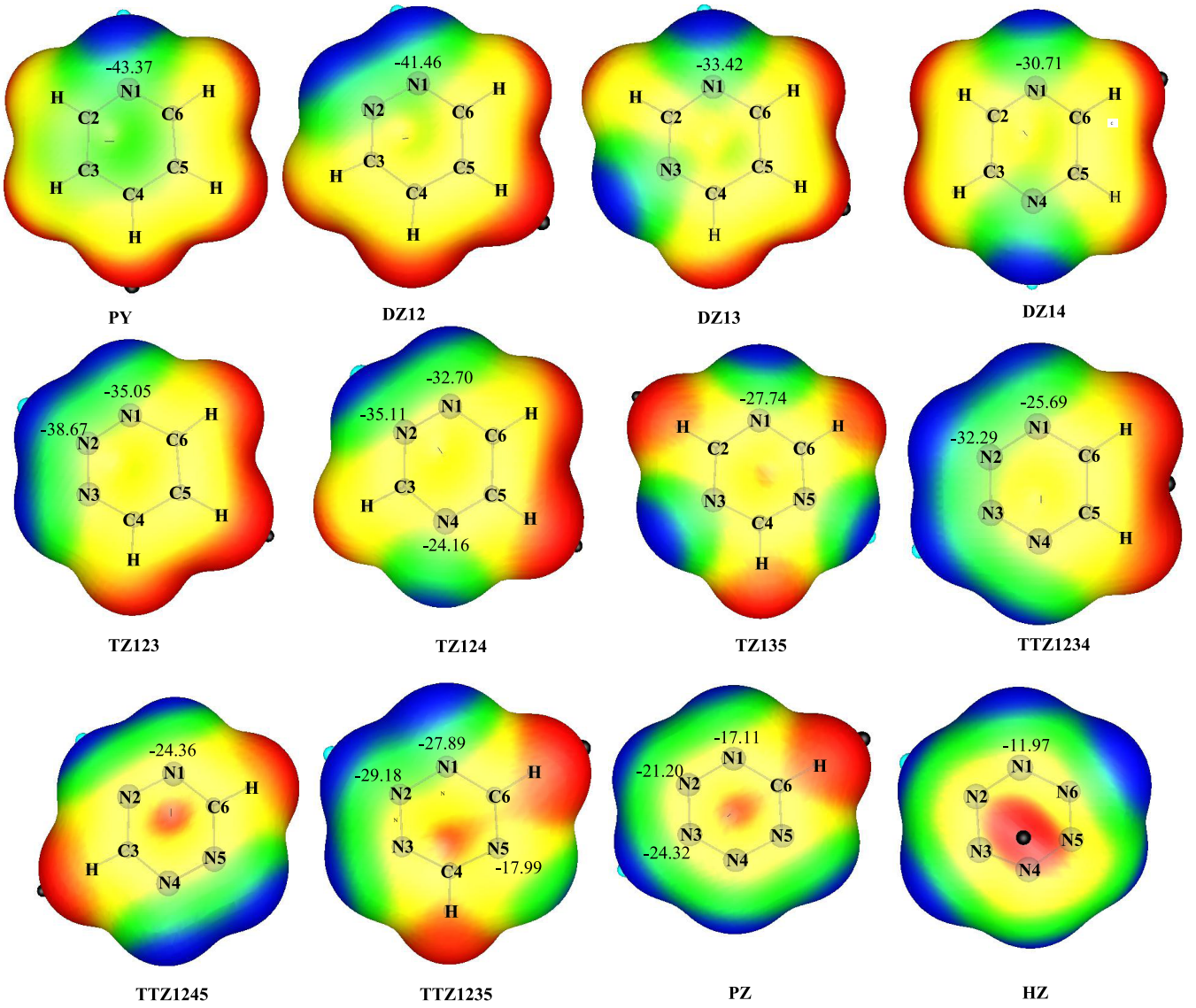

Figure 4. Molecular electrostatic potential (MEP) of azines at MP2/aug-cc-pVDZ level. The numerical values shown are the MEP values (in kcal/mol) for the corresponding nitrogen atoms.

H···O_W HB angle in these complexes lie in the range of 115−122°, which is in agreement with the IUPAC definition according to which the X−H···Y angle should be greater than 110° for an interaction to be characterized as a HB.

In type **WIV** complexes (shown in Figure S1), the oxygen of water acts as a HB acceptor toward C−H bond of azine. These complexes involve single HB formation with C−H···O_W interaction. The stabilization energy for these complexes depends on the number of N atoms and position of C−H bond relative to the nitrogen atom. The order of stabilization energy in these complexes is: **TZ123** > **TZ124** > **DZ12** > **DZ13** > **DZ14** > **PY**, which shows that C−H HB donor ability increases with increase in the aza substitution. The C−H···O_W HB angles in these complexes lie in the range of 178−180°. The **WIV** complexes of **DZ12** and **TZ123** have higher ΔE_{BSSE} in which the C−H bond involved in HB interaction is meta and para to the nitrogen atom, whereas **WIV** complexes of **DZ14** and **TZ124** have lower ΔE_{BSSE} values in which the C−H bond involved in HB interaction is ortho to the nitrogen atom, which clearly shows that C−H bond meta or para to a nitrogen atom forms a more stable complex relative to C−H bond ortho to a nitrogen atom. The **WIV** complexes are 0.02−0.30 kcal/mol less stable in comparison to their respective **WIII** complexes.

2.2. Vibrational Properties of a Hydrogen-Bond Donor. Table 1 displays the change in HB donor (Δd in Å) and shifts of stretching frequencies ($\Delta\nu$ in cm^{-1}) of the HB donor group upon complex formation relative to monomers. Upon complex formation, O−H of water as a HB donor in a conventional N···H−O_W HB is usually red-shifted due to which O−H frequency decreases and there is lengthening of the O−H bond whereas in contrast to unconventional C−H···O_W HB, C−H as a HB donor usually is blue-shifted due to which the frequency of C−H bond increases and there is shortening of C−H bond. In type **WI** complexes involving single N···H−O_W interaction, the order of $\Delta\nu$ for O−H bond is as follows: **PY** > **TZ** > **TTZ** > **PZ** > **HZ**, which elucidates the fact that $\Delta\nu$ decreases as aza substitution increases in the ring. This can be understood in terms of electron density transfer, i.e., $n_N \rightarrow \sigma^*_{O-H}$ orbital interaction. Upon continuous addition of nitrogen atoms, there is a regular decrease in the electron density shift from the nitrogen atom of azine to σ^* orbital of O−H bond of water, which leads to a decrease in the red shift of O−H_W bond.

DOI: 10.1021/acsomega.8b03496
ACS Omega 2019, 4, 8112−8121

The order of $\Delta\nu$ correlates well with the change in O−H bond length and hydrogen-bond distance formed in these complexes. The shorter the N···H−O_W HB distance (r), larger will be the change in the HB donor length $_W$O−H (Δd) and higher will be the stretching frequency shift ($\Delta\nu$). Furthermore, stabilization energy of these complexes also corroborates with the shift in stretching frequency. The Δd and $\Delta\nu$ values for red-shifted O−H bond are relatively higher in complexes involving single N···H−O_W interaction in comparison with complexes in which the second HB is also associated with the former complexes, as reflected from the comparison of type **WI** (N···H−O_W) and type **WII** (C−H···O_W and N···H−O_W) complexes. The Δd and $\Delta\nu$ for blue-shifted stretches are small in magnitude in a bifurcated structure with two C−H···O_W interactions but a similar variation is larger in complexes involving single C−H···O_W interaction, which is evident from the comparison of type **WIII** and **WIV** complexes.

2.3. Natural Bond Orbital (NBO) Analysis. NBO is an excellent tool for investigation of second-order delocalization energies. The results of NBO analysis (Table S2) show that lone pair electrons on a pyridinic nitrogen atom are shifted to σ^* antibonding orbital of HB donor $_W$O−H in type **WI** and **WII** complexes under study except **DZ14-WII**, **TZ123-WI**, and **TZ123-WII**. In the latter complexes, lone pair of electrons are transferred from pyridinic nitrogen atom to hydrogen atom. The decrement in $E^{(2)}$ values for $n_N \rightarrow \sigma^*_{O-H}$ orbital interactions with inclusion of nitrogen atoms in the ring, as seen in type **WI** and **WII** complexes, displays that continuous augmentation of nitrogen atoms in the ring reduces the population of electron density shift from lone pair on pyridinic nitrogen (N) to the σ^* antibonding O−H orbital of water and is also in consonance with a decrease in red shift of O−H stretching vibration upon gradual addition of nitrogen atoms in the ring. Rehybridization enhances the s character of carbon hybrid orbital of C−H bond with continuous incorporation of nitrogen atoms in the ring, as seen in type **WIII** and **WIV** complexes, which leads to shortening and contraction of C−H···O_W HB. The $n_N \rightarrow \sigma^*_{O-H}$ orbital interaction in type **WII** complexes has $E^{(2)}$ values lower in comparison with similar orbital interactions in type **WI**. It is worth noticing that the $E^{(2)}$ values for two $n_O \rightarrow \sigma^*_{C-H}$ orbital interactions are lesser to a large extent in complexes of type **WIII** in comparison with their counterpart complexes of type **WIV**, which possess single $n_O \rightarrow \sigma^*_{C-H}$ orbital interactions. Section S1 provides an analysis for charge transfer and atomic charges on atoms involved in HB formation.

2.4. Topological Analysis. Atoms in molecules (AIM) provide an elegant approach to study the concept of hydrogen-bonding interactions.

The hydrogen-bonded molecular geometries of azine−water complexes at MP2/aug-cc-pVDZ have been employed to calculate the topological properties; see Section S2 for description of topological parameters. The AIM molecular graphs of the complexes are displayed in Figure 3 where small red balls indicate bond critical points and yellow balls indicate ring critical points. As seen in Table S3, all HBs in complexes under study satisfy Koch and Popelier's criteria with ρ_c and $\nabla^2\rho_c$ of (3, −1) values well within the respective ranges 0.005−0.029 au and 0.028−0.102 au. The ρ_c and $\nabla^2\rho_c$ values of **WI** and **WII** complexes follow the order **PY** > **DZ** > **TZ** > **TTZ** > **PZ** > **HZ**, which supports the fact that the tendency of the pyridinic nitrogen atom of azine to play the role of an HB acceptor decreases with increase in the aza substitution. The order of ρ_c and $\nabla^2\rho_c$ of (3, −1) values in **WIII** and **WIV** complexes follow the order **TTZ** > **TZ** > **DZ** > **PY**, which authenticates the fact that C−H HB donor ability decreases as the aza substitution decreases. A good correlation is found to exist between ρ_c and ΔE_{BSSE} values for complexes under study (Figure S3). Also, there exists a linear relationship between $\nabla^2\rho_c$ and ΔE_{BSSE} values (Figure S4).

2.5. Analysis of Molecular Electrostatic Potential (MEP) and Proton Affinity (PA). The study of molecular electrostatic potential (MEP) is a useful descriptor for predicting the reactivity of each of the unique nitrogen atoms in the azines. It provides important information about the HB interaction, which is largely an electrostatic phenomenon. Figure 4 depicts the contour maps of MEP of azines displaying the electrostatic potential values of ring nitrogens; red and blue regions indicate positive and negative MEP sites, respectively. The proton affinity (PA) of a molecule can easily be related to nucleophilicity of the basic site, and it provides useful information about the basicity and reactivity of different nitrogens present in the azines. The PA values of different nitrogen atoms in the azines are shown in Table 2. Both MEP and PA values reflect that the basicity of azine reduces with progressive addition of nitrogen atoms in the ring and with increasing distance between two nitrogen atoms. For instance, the inclusion of a second nitrogen atom within the aromatic ring implies the reduction in the proton affinity values by 3.8, 11.3, and 12.6 kcal/mol and MEP values by 1.91, 9.95, and 12.66 kcal/mol for ortho (**DZ12**), meta (**DZ13**), and para (**DZ14**) substitution, respectively, with respect to **PY**. It is observed that **DZ12** is the most basic among diazines and likewise **TZ123** and **TTZ1234** are the most basic among triazines and tetrazines, respectively.

Table 2. Proton Affinity Values at Different Nitrogen Atoms of Azines (in kcal/mol)

azines	protonated center	proton affinity
PY	N1	218.0
DZ12	N1	214.2
DZ13	N1	206.7
DZ14	N1	205.4
TZ123	N1	200.4
	N2	206.8
TZ124	N1	201.5
	N2	202.0
	N4	191.8
TZ135	N1	195.2
TTZ1234	N1	195.8
	N2	204.6
TTZ1235	N1	199.2
	N2	201.2
	N5	182.0
TTZ1245	N1	200.1
PZ	N1	170.2
	N2	180.9
	N3	183.3
HZ	N1	168.3

The most negative potential with the notation V_{min} is used to diagnose the electron-rich site of the molecule, whereas the most positive potential denoted by V_{max} is used to recognize the electron-deficient site of the molecule (Table S1). The electronic changes occurring during the HB formation can be clearly understood by comparing V_{min} values of isolated azines

DOI: 10.1021/acsomega.8b03496
ACS Omega 2019, 4, 8112−8121

with V_{min} values of azines in the complex (designated as V'_{min}). Hence, electronic reorganization during the HB formation can be gauged as $\Delta V_{min} = V'_{min} - V_{min}$ and these MEP parameters are summarized in Table S2; see Section S3 for a detailed analysis.

2.6. Symmetry-Adapted Perturbation Theory (SAPT). SAPT has been carried out to decompose the stabilization energy into contributing factors. This method is employed to partition the stabilization energy into physically meaningful components, like electrostatic (E_{els}), induced (E_{ind}), dispersion (E_{disp}), exchange (E_{exch}) interactions, etc. The E_{els}, E_{ind}, and E_{disp} components are attractive energy terms stabilizing the complexes, whereas E_{exch} component is repulsive. The term $\delta E_{int,r}^{HF}$ is calculated as the difference between the Hartree−Fock interaction energy and the sum of all SAPT energy terms (up to the second order) that do not include any correlation effects. The SAPT components for the complexes of azines with water in MP2/aug-cc-pVDZ basis set are reported in Table S4. Generally, all energy terms increase with sequential addition of nitrogen atoms in the azine ring. A larger role of the induction term in comparison with the dispersion term is found in red-shifted hydrogen-bonded complexes of type **WI** and **WII**, whereas the opposite picture has been seen in blue-shifted hydrogen-bonded type **WIII** and **WIV** complexes. The percentage stability due to electrostatic component is higher in complexes involving single C−H···O_W interaction (65.12−66.36%) relative to that in complexes involving single N···H−O_W interaction (56.27−57.17%). The percentage contribution of the E_{ind} (22.79−23.73%) and E_{disp} (19.38−20.13%) components in complexes involving single N···H−O_W interaction suggests the relatively higher contribution of the E_{ind} term over the E_{disp} term, whereas the percentage contribution of the E_{ind} (15.37−16.68%) and E_{disp} (17.58−18.72%) components in complexes involving single C−H···O_W interaction is nearly the same.

3. CONCLUSIONS

We have performed MP2 and wB97XD calculations at aug-cc-pVDZ level to study the hydrogen-bonding interaction between water and aromatic heterocyclic azines. The results of stabilization energies, vibrational frequencies, NBO, MEP, and SAPT calculations support the following statements.

1. The HB acceptor ability of the pyridinic nitrogen atom of azine is found to be decreased in the order **PY** > **DZ** > **TZ** > **TTZ** > **PZ** > **HZ** during complexation with water. Infact, the inclusion of the subsequent addition of nitrogen atoms in the ring is accompanied by an inductive effect due to N−N lone pair interactions, which reduces the tendency of binding a proton. Thus, the basicity of a pyridinic nitrogen atom of azine reduces as we move from **PY** to **HZ**, which is also in consonance with proton affinity values. Further, the complexes in which the basic center is directly bonded to a nitrogen atom, such as **DZ12-WII**, **TZ123-WII**, and **TTZ1234-WII**, reveal strong hydrogen-bonded interaction in comparison with complexes in which the basic center is not directly bonded to a nitrogen atom, such as **DZ13-WII**, **DZ14-WII**, and **TZ135-WII**, which will be manifested again when considering proton affinity values.
2. The HB donor ability of the C−H bond of azine is found to be increased in the order **PY** < **DZ** < **TZ** < **TTZ**. Indeed, the successive aza substitution makes the C−H bond of azine more acidic and thus the HB donor ability of the C−H bond gets increased on moving from **PY** to **TTZ**. Moreover, it is observed that the C−H bond of azine acts as a better HB donor when it is at the meta or para position to aza nitrogen relative to the ortho-positioned nitrogen atom.
3. Continuous increments in the red-shift values of O−H_W bond and decrement in the blue-shift values of C−H_{azine} bond are observed on moving from **PY** to **TTZ**, which can be explained on the basis of hyperconjugative O−H bond lengthening and rehybridization-promoted C−H bond shortening, respectively.

4. COMPUTATIONAL METHODS

Ab initio calculations are carried out through Gaussian 09 software.[44] Geometry optimization of azines and their corresponding complexes with water are performed at the second-order Møller−Plesset perturbation (MP2) level in combination with aug-cc-pVDZ basis set. For comparison purpose, density functional theory with dispersion calculations at the wB97XD level was also applied in conjuction with the aug-cc-pVDZ set. Stabilization energy (ΔE_{BSSE}) is predicted as equal to the difference in energy between each complex and sum of isolated monomers employing the counterpoise (CP) method of Boys and Bernardi.[45] NBO analysis was performed at wB97XD/aug-cc-pVDZ to analyze the atomic charges, charge transfer, and $E^{(2)}$ values within Gaussian 09 package.[46] AIM analysis in molecules using the AIM2000 suite of program is employed to determine the topological and energetical properties at BCPs and RCPs.[47] The molecular electrostatic potential (MEP) was calculated using the WFA surface analysis suite.[48,49] SAPT calculations for the HB complexes under study are calculated by the use of GAMESS package linked to the SAPT 2012.2 code, to decompose the total stabilization energy into four fundamental components, namely, electrostatic, induction, dispersion, and exchange energies.[50−52]

■ ASSOCIATED CONTENT

Supporting Information

The Supporting Information is available free of charge on the ACS Publications website at DOI: 10.1021/acsomega.8b03496.

MEP parameters V_{max} and V_{min} of azines (Table S1); second-order delocalization energies $E^{(2)}$ at wB97XD/aug-cc-pVDZ (L1) and MP2/aug-cc-pVDZ (L2) levels, atomic charges and the amount of charge transfer from azines to water at L1 level and MEP parameters V'_{min} and ΔV_{min} in complexes of azine with water at L2 level (Table S2); topological and energetic properties at the bond critical points (bcps) and ring critical points (rcps) for the azine−water complexes evaluated at L2 theoretical level using AIM analysis (Table S3); SAPT components of the stabilization energy for complexes of azines with water evaluated at L2 level (Table S4); optimized parameters for azine−water complexes at L1 and L2 levels (Tables S5−S19); optimized geometries of 1:1 hydrogen-bonded complexes of azines with water at L2 level (type **WIII** and **WIV**) (Figure S1); AIM molecular graphs of complexes of azines with water at L2 level (Figure S2); plot of the relation between stabilization energy (ΔE_{BSSE}) and ρ_c (Figure S3); plot of the relation between stabilization energy (ΔE_{BSSE}) and $\nabla^2\rho_c$ (Figure S4); elaborate

DOI: 10.1021/acsomega.8b03496
ACS Omega 2019, 4, 8112−8121

discussion of charge transfer and atomic charges (Section S1), topological parameters (Section S2), V_{max} and V_{min} analysis (Section S3) (PDF)

AUTHOR INFORMATION

Corresponding Author

*E-mail: nehaomnamah@gmail.com.

ORCID

Neha Chopra: 0000-0002-8545-2772

Notes

The authors declare no competing financial interest.

ACKNOWLEDGMENTS

The authors are highly grateful to the Council of Scientific and Industrial Research (CSIR) and University Grants Commission (UGC) New Delhi, India, for the financial assistance.

REFERENCES

(1) Müller-Dethlefs, K.; Hobza, P. Noncovalent Interactions: A Challenge for Experiment and Theory. *Chem. Rev.* **2000**, *100*, 143−167.

(2) Muller-Dethlefs, K.; Hobza, P. *Non-Covalent Interactions: Theory and Experiment*, 1st ed.; RSC: Cambridge, 2010; pp 1−238.

(3) Černý, J.; Hobza, P. Non-covalent interactions in biomacromolecules. *Phys. Chem. Chem. Phys.* **2007**, *9*, 5291−5303.

(4) Robertson, E. G.; Simons, J. P. Getting Into Shape: Conformational and Supramolecular Landscapes in Small Biomolecules and their Hydrated Clusters. *Phys. Chem. Chem. Phys.* **2001**, *3*, 1−18.

(5) de Vries, M. S.; Hobza, P. Gas-phase Spectroscopy of Biomolecular Building Blocks. *Annu. Rev. Phys. Chem.* **2007**, *58*, 585−612.

(6) Garand, E.; Kamrath, M. Z.; Jordan, P. A.; Wolk, A. B.; Leavitt, C. M.; McCoy, A. B.; Miller, S. J.; Johnson, M. A. Determination of Noncovalent Docking by Infrared Spectroscopy of Cold Gas-Phase Complexes. *Science* **2012**, *335*, 694−698.

(7) Sowerby, S. J.; Heckl, W. M. The Role of Self-Assembled Monolayers of the Purine and Pyrimidine Bases in the Emergence of Life. *Origins Life Evol. Biospheres* **1998**, *28*, 283−310.

(8) Grabowski, S. J. Ab Initio Calculations on Conventional and Unconventional Hydrogen Bonds-Study of the Hydrogen Bond Strength. *J. Phys. Chem. A* **2001**, *105*, 10739−10746.

(9) Kryachko, E. S.; Zeegers-Huyskens, T. Theoretical Study of the CH···O Interaction in Fluoromethanes·H2O and Chloromethanes·H2O Complexes. *J. Phys. Chem. A* **2001**, *105*, 7118−7125.

(10) Scheiner, S.; Kar, T. Effect of Solvent upon CH···O Hydrogen Bonds with Implications for Protein Folding. *J. Phys. Chem. B* **2005**, *109*, 3681−3689.

(11) Manikandan, K.; Ramakumar, S. The Occurrence of COH...O Hydrogen Bonds in α-Helices and Helix Termini in Globular Proteins. *Proteins: Struct., Funct., Bioinf.* **2004**, *56*, 768−781.

(12) Horowitz, S.; Trievel, R. C. Carbon-Oxygen Hydrogen Bonding in Biological Structure and Function. *J. Biol. Chem.* **2012**, *287*, 41576−41582.

(13) Yesselman, J. D.; Horowitz, S.; Brooks, C. L., III; Trievel, R. C. Frequent side chain methyl carbon-oxygen hydrogen bonding in proteins revealed by computational and stereochemical analysis of neutron structures. *Proteins* **2015**, *83*, 403−410.

(14) Steiner, T.; Saenger, W. Geometry of C-H···O Hydrogen Bonds in Carbohydrate Crystal Structures. Analysis of Neutron Diffraction Data. *J. Am. Chem. Soc.* **1992**, *114*, 10146−10154.

(15) Li, Q.; Huang, F.-Q.; Hu, J. D.; Zhao, K.-Q. Theoretical Study on the Structures and Properties of Hydrogen Bonding Complexes between Diazines and Water. *Chin. J. Chem.* **2006**, *24*, 1700−1703.

(16) Li, Q.; Hu, J. D.; Zhao, K.-Q. DFT Study of Hydrogen-Bonded 1,3,5-Triazine-Water Complexes. *Chin. J. Chem.* **2007**, *25*, 1078−1081.

(17) Li, Q.; Huang, F.-Q. Hydrogen Bonding Structure and Many Body Interactions in 1,3,5-Triazine−$(Water)_3$ and 1,2,4-Triazine−$(Water)_3$ Complexes. *Int. J. Quantum Chem.* **2007**, *107*, 567−573.

(18) Yun-Chun, L.; Quan, L.; Ke-Qing, Z. A computational study of hydrogen bonding complexes between 1,2,3-triazine and water. *J. Mol. Struct: Theochem.* **2006**, *766*, 83−86.

(19) Li, Q.; Huang, F.-Q. Many-body Interaction in 1,2,3-Triazine-$(water)_3$ Complex. *Chin. J. Chem.* **2005**, *23*, 1314−1318.

(20) Li, Q.; Huang, F.-Q.; H; Hu, J.-D.; Zhao, K.-Q. Hydrogen-bonding Interaction of 1,2,3-triazine-waters Complexes. *Chin. J. Chem. Phys.* **2006**, *19*, 401−405.

(21) Cai, Z. -L; Reimers, J. R. The First Singlet (n,π*) and (π,π*) Excited States of the Hydrogen-Bonded Complex between Water and Pyridine. *J. Phys. Chem. A* **2002**, *106*, 8769−8778.

(22) Schlücker, S.; Koster, J.; Singh, R. K.; Asthana, B. P. Hydrogen-Bonding between Pyrimidine and Water: A Vibrational Spectroscopic Analysis. *J. Phys. Chem. A* **2007**, *111*, 5185−5191.

(23) Chopra, N.; Kaur, D.; Chopra, G. Nature and Hierarchy of Hydrogen-Bonding Interactions in Binary Complexes of Azoles with Water and Hydrogen Peroxide. *ACS Omega* **2018**, *3*, 12688−12702.

(24) Chopra, N.; Kaur, D.; Chopra, G. Hydrogen bonded complexes of oxazole family: electronic structure, stability, and reactivity aspects. *Struct. Chem.* **2018**, *29*, 341−357.

(25) Rusu, V. H.; Ramos, M. N.; Dasilva, J. B. P. Hydrogen Bonds Between Hydrogen Fluoride and Aromatic Azines: An Ab Initio Study. *Int. J. Quantum Chem.* **2006**, *106*, 2811−2817.

(26) Chaubey, A.; Pandeya, S. N. Pyridine" A Versatile Nucleuse in Pharmaceutical Field. *Asian J. Pharm. Clin. Res.* **2011**, *4*, 5−8.

(27) Dias, L. R. S.; Santos, M. B.; de Albuquerque, S.; Castro, H. C.; de Souza, A. M. T.; Freitas, A. C. C.; DiVaio, M. A. V.; Cabral, L. M.; Rodrigues, C. R. Synthesis, in vitro evaluation, and SAR studies of a potential antichagasic 1H-pyrazolo[3,4-b]pyridine series. *Bioorg. Med. Chem.* **2007**, *15*, 211−219.

(28) Choudhari, P. B.; Mulani, A. K.; Ingale, K. B.; Bhatia, N. M.; Bhatia, M. S. Synthesis and QSAR analysis of 5-substituted (arylmethylene) pyridin-2-amine derivatives as potential antibacterials. *Int. J. Drug Discovery* **2009**, *1*, 1−9.

(29) Chezal, J. M.; Paeshuyse, J.; Gaumet, V.; Canitrot, D.; Maisonial, A.; Lartigue, C.; Gueiffier, A.; Moreau, E.; Teulade, J. C.; Chavignon, O.; Neyts, J. Synthesis and antiviral activity of an imidazo[1,2-a]pyrrolo[2,3-c]pyridine seriesagainst the bovine viral diarrhea virus. *Eur. J. Med. Chem.* **2010**, *45*, 2044−2047.

(30) Asif, M.; Singh, A.; Ratnakar, L. Antimicrobial Agents: Brief Study of Pyridazine Derivatives against Some Phathogenic Microrganisms. *J. Pharm. Res.* **2011**, *4*, 664−667.

(31) Guan, L.-P.; Sui, X.; Deng, X.-Q.; Quan, Y.-C.; Quan, Z.-S. Synthesis and anticonvulsant activity of a new 6-alkoxy-[1,2,4]triazolo-[4,3-b]pyridazine. *Eur. J. Med. Chem.* **2010**, *45*, 1746−1752.

(32) Asif, M.; Singh, A. Exploring Potential, Synthetic Methods and General Chemistry of Pyridazine and Pyridazinone: A Brief Introduction. *Int. J. ChemTech Res.* **2010**, *2*, 1112−1128.

(33) Cao, S.; Qian, X.; Song, G.; Chai, B.; Jiang, Z. Synthesis and Antifeedant Activity of New Oxadiazolyl 3(2*H*)-Pyridazinones. *J. Agric. Food Chem.* **2003**, *51*, 152−155.

(34) Abouzid, K.; Hakeem, M. A.; Khalil, O.; Maklad, Y. Pyridazinone derivatives: Design, synthesis, and in vitro vasorelaxant activity. *Bioorg. Med. Chem.* **2008**, *16*, 382−389.

(35) Taylor, E. C.; Liu, B. A New and Efficient Synthesis of Pyrrolo[2,3-*d*]pyrimidine Anticancer Agents: Alimta (LY231514, MTA), Homo-Alimta, TNP-351, and Some Aryl 5-Substituted Pyrrolo[2,3-*d*]pyrimidines. *J. Org. Chem.* **2003**, *68*, 9938−9947.

(36) Chatterjee, S.; Wang, F. How different is pyrimidine as a core component of DNA base from its diazine isomers: A DFT study? *Int. J. Quantum Chem.* **2016**, *116*, 1836−1845.

(37) Raczyńska, E. D.; Makowski, M.; Hallmann, M.; Kaminska, B. Geometric and energetic consequences of prototropy for adenine and its structural models − a review. *RSC Adv.* **2015**, *5*, 36587−36604.

(38) El-Hamdi, M.; Tiznado, W.; Poater, J.; Sola, M. An Analysis of the Isomerization Energies of 1,2-/1,3-Diazacyclobutadiene, Pyrazole/

DOI: 10.1021/acsomega.8b03496
ACS Omega 2019, 4, 8112−8121

Imidazole, and Pyridazine/Pyrimidine with the Turn-Upside-Down Approach. *J. Org. Chem.* **2011**, *76*, 8913−8921.
(39) Lagoja, I. M. Pyrimidine as a Constituent of Natural Biologically Active Compounds. *Chem. Biodiversity* **2005**, *2*, 1−50.
(40) Amir, M.; Javed, S. A.; Kumar, H. Pyrimidine as Antiinflammatory Agent: A Review. *Indian J. Pharm. Sci.* **2007**, *69*, 337−343.
(41) Anupama; Khan, I.; Singh, B. Synthesis of Biologically Important s-Triazine Based Chalcones. *Int. J. Pharm. Sci. Res.* **2015**, *6*, 3209−3214.
(42) Ni, Z.; Zhou, L.; Li, X.; Zhang, J.; Dong, S. Tetrazine- Containing Amino Acid for Peptide Modification and Live Cell Labeling. *PLoS One* **2015**, *10*, No. e0141918.
(43) Shahi, A.; Arunan, E. Why are Hydrogen Bonds Directional? *J. Chem. Sci.* **2016**, *128*, 1571−1577.
(44) Frisch, M. J.; Trucks, G. W.; Schlegel, H. B.; Scuseria, G. E.; Robb, M. A.; Cheeseman, J. R.; Scalmani, G.; Barone, V.; Mennucci, B.; Petersson, G. A.; Nakatsuji, H.; Caricato, M.; Li, X.; Hratchian, H. P.; Izmaylov, A. F.; Bloino, J.; Zheng, G.; Sonnenberg, J. L.; Hada, M.; Ehara, M.; Toyota, K.; Fukuda, R.; Hasegawa, J.; Ishida, M.; Nakajima, T.; Honda, Y.; Kitao, O.; Nakai, H.; Vreven, T.; Montgomery, J. A.; Peralta, J. E.; Ogliaro, F.; Bearpark, M.; Heyd, J. J.; Brothers, E.; Kudin, K. N.; Staroverov, V. N.; Kobayashi, R.; Normand, J.; Raghavachari, K.; Rendell, A.; Burant, J. C.; Iyengar, S. S.; Tomasi, J.; Cossi, M.; Rega, N.; Millam, J. M.; Klene, M.; Knox, J. E.; Cross, J. B.; Bakken, V.; Adamo, C.; Jaramillo, J.; Gomperts, R.; Stratmann, R. E.; Yazyev, O.; Austin, A. J.; Cammi, R.; Pomelli, C.; Ochterski, J. W.; Martin, R. L.; Morokuma, K.; Zakrzewski, V. G.; Voth, G. A.; Salvador, P.; Dannenberg, J. J.; Dapprich, S.; Daniels, A. D.; Farkas, O.; Foresman, J. B.; Ortiz, J. V.; Cioslowski, J.; Fox, D. J. *Gaussian 09*, revision B01; Gaussian, Inc.: Wallingford CT, 2009.
(45) Merrick, J. P.; Moran, D.; Radom, L. An Evaluation of Harmonic Vibrational Frequency Scale Factors. *J. Phys. Chem. A* **2007**, *111*, 11683−11700.
(46) Reed, A. E.; Curtiss, L. A.; Weinhold, F. Intermolecular interactions from a natural bond orbital, donor-acceptor viewpoint. *Chem. Rev.* **1988**, *88*, 899.
(47) Bader, R. F. W. *Atoms in Molecules - A Quantum Theory*; Oxford University Press: Oxford, 1990.
(48) Bulat, F. A.; Toro-Labbe, A.; Brinck, T.; Murray, J. S.; Politzer, P. Quantitative analysis of molecular surfaces: areas, volumes, electrostatic potentials and average local ionization energies. *J. Mol. Model.* **2010**, *16*, 1679−1691.
(49) Politzer, P.; Truhlar, D. G. *Chemical Applications of Atomic and Molecular Electrostatic Potentials*; Plenum: New York, 1981; pp 7−28.
(50) Jeziorski, B.; Moszyński, R.; Szalewicz, K. Perturbation Theory Approach to Intermolecular Potential Energy Surfaces of van der Walls Complexes. *Chem. Rev.* **1994**, *94*, 1887.
(51) Moszyński, R. Symmetry-adapted perturbation theory for the calculation of Hartree-Fock interaction energies. *Mol. Phys.* **1996**, *88*, 741−758.
(52) Bukowski, R.; Cencek, W.; Jankowski, P.; Jeziorska, M.; Jeziorski, B.; Korona, T.; Kucharski, S. A.; Lotrich, V. F.; Misquitta, A. J.; Moszyński, R.; Patkowski, K.; Podeszwa, R.; Rob, F.; Rybak, S.; Szalewicz, K.; Williams, H. L.; Wheatley, R. J.; Wormer, P. E. S.; Żuchowski, P. S. *SAPT2012: An Ab Initio Program for Many-Body Symmetry-Adapted Perturbation Theory Calculations of Intermolecular Interaction Energies*; University of Delaware and University of Warsaw, 2012.

DOI: 10.1021/acsomega.8b03496
ACS Omega 2019, 4, 8112−8121